Article

Oxidative potential and persistent free radicals in dust storm particles and their associations with hospitalization

Linjun Qin[1,2,3], Lili Yang [1,2] ✉, Ling Liu[4], Shilu Tong [5], Qian Liu [1,2], Gang Li[1,2], Haiyan Zhang[3], WuYuxin Zhu[1,2,3], Guorui Liu [1,2,3] ✉, Minghui Zheng [1,2,3] & Guibin Jiang[1,2,3]

Sand and dust storms (SDS) can cause adverse health effects, with the oxidative potential (OP) and environmentally persistent free radicals (EPFRs) inducing oxidative stress. We mapped the OP and EPFRs concentrations at 1735 sites in China during SDS periods using experimental data for 2021–2023 and a random forest model. We examined 855,869 hospitalizations during SDS events for 2015–2022 in Beijing, China. An integrated exposure–response model was used to estimate the association between OP and EPFRs and hospitalization during SDS. EPFRs were strongly associated with circulatory (3.05%; 95% confidence interval [CI]: 1.01%, 4.08%) and respiratory (2.02%; 95% CI: 1.01%, 4.08%) diseases with each increase of 10^{12} spins/m^3. The OP effects on circulatory (3.52%; 95% CI: 2.13%, 4.92%) and respiratory diseases (2.08%; 95% CI: 1.13%, 3.04%) with each increase of 0.2 nmol/min/m^3 were also statistically significant. Additionally, 20.47% and 27.26% of all-cause hospitalizations were attributable to OP and EPFRs exposure, respectively. This knowledge could be used to develop effective sand and dust risk prevention in dust-prone countries.

Dust storms are meteorological hazards that arise when large amounts of sand and dust from the Earth's surface are lifted into the troposphere by cyclones[1,2]. These extreme weather events occur frequently in Africa, Central Asia, North America, and Australia[3]. During dust storms, cyclones produce turbulent mixing and convective updrafts that lead to transmission of dust particles across vast geographical ranges and international borders. Global dust emissions are estimated at ~1200 Tg/yr[3,4]. Dust storms typically occur in arid and semi-arid regions. The dust from these storms can have a significant impact on the health and wellbeing of populations in urban areas or other regions beyond the areas where dust storms are generated. In the spring of 2021–2023, Asia was struck by several enormous dust storm events[2,5,6]. The observed peak concentrations of inhalable particulate matter (PM$_{10}$) during the event occurred from March 14–15, 2021, and was

>9985 μg/m^3 in Ulanqab, and >7400 μg/m^3 in Beijing[2]. In 2023, more than 15 provinces in China were affected by severe sandstorms. These intense sandstorms had profound implications and attracted significant attention.

Dust storms are associated with a variety of adverse health outcomes in humans[7–11]. For example, epidemiological studies have reported positive associations of dust events with human mortality and hospital admissions for circulatory and respiratory diseases[7,12]. However, previous epidemiological studies have predominantly assessed the adverse effects of particulate matter (PM) on human health using the mass concentrations during the sand and dust storm (SDS) events[13,14]. Recent studies have shown that low levels of atmospheric PM can also have detrimental effects, but the PM concentrations alone cannot fully explain the effect of PM on health[13–15]. The

[1]State Key Laboratory of Environmental Chemistry and Ecotoxicology, Research Center for Eco-Environmental Sciences, Chinese Academy of Sciences, Beijing 100085, China. [2]College of Resources and Environment, University of Chinese Academy of Sciences, Beijing 100190, China. [3]Institute of Environment and Health, Hangzhou Institute for Advanced Study, University of Chinese Academy of Sciences, Hangzhou 310024, China. [4]Peking University Third Hospital, Beijing 100191, China. [5]Queensland University of Technology, Brisbane, QLD, Australia. ✉e-mail: llyang@rcees.ac.cn; grliu@rcees.ac.cn

adverse effects of critical components in PM are currently unclear. This knowledge could help with understanding the underlying mechanisms of dust particles on human health.

Oxidative stress has emerged as a mechanism that underlies the toxic effects of PM pollution[16,17]. Consequently, PM components and metrics that induce oxidation stress in the human body are of concern[18]. Redox-active PM species that have oxidative potential (OP), which are represented by metals and organic pollutants, can catalyze the generation of reactive oxygen species (ROS) in vivo and lead to oxidative stress[18,19]. The OP is associated with adverse health effects during PM pollution events[18–21]. It has been suggested that the OP is one of many possible drivers of the acute health effects of PM, but the link is unclear[19]. Few studies have explored associations between OP and diseases during SDS periods. Environmentally persistent free radicals (EPFRs), which are emerging contaminants that are attached to and stabilized on PM, can also induce oxidative stress in the human body[22–26]. These organic free radicals are formed through electron abstraction from organic pollutants on PM. The structure of PM causes pronounced steric hindrance towards these organic radicals, which ultimately leads to the formation of EPFRs[27–29]. EPFRs have both radical activity and organic pollutant stability. The EPFRs-containing PM redox cycle can produce ROS[23,30,31], which contributes to the oxidative stress and OP levels. Adverse human health effects caused by EPFRs bound to PM have been increasingly recognized. It has been suggested that EPFRs might explain why non-smokers suffer from similar lung diseases to smokers[32,33]. The associations of EPFRs on PM with health outcomes during SDS periods need further exploration. Studies to assess the associations of health outcomes with OP and EPFRs are urgently needed.

There is a lack of data for OP and EPFRs concentrations during practical SDS events. Obtaining such data requires in situ sampling of atmospheric PM, sample transportation to the laboratory, and offline detection[19,22]. The complexity of sample collection in a moving SDS makes the detection of OP and EPFRs time-consuming and labor-intensive. To clarify the distribution and evolution of OP and EPFRs throughout a storm's progression, simultaneous sample collection is required at multiple sites through which the storm may pass. All those requirements make the analysis of the transportation and distribution of OP and EPFRs in dust storms very challenging. Using available air quality data and meteorological parameters to conduct gridded predictions of the OP and EPFR concentrations, which can be easily achieved using established monitoring systems, may be a feasible alternative for obtaining the OP and EPFR concentrations. Therefore, it is essential to establish a model that can utilize available air quality data and meteorological parameters to accurately quantify the OP and EPFRs concentrations.

In this study, we conducted synchronous PM sample collection over a 3 year period in nine cities during the SDS events that occurred in China between 2021 and 2023. In total, 190 dust particle samples were collected and tested for the OP and EPFRs bound to the dust storm particles. Using a database of measured OP and EPFRs concentrations, and available air quality data and meteorological parameters, machine learning models for predicting the OP and EPFRs concentrations were established to map the OP and EPFR distributions across China during the SDS. We selected Beijing as a representative dust-prone megacity, and used comprehensive data on human diseases during dust storm events. By linking these diseases to the OP and EPFRs in dust storm particles, we aimed to gain insight into the contributions of the OP and EPFRs to the observed health effects.

Results
Random Forest modeling
Figure 1 shows the random forest (RF) modeling workflow used in this study. This encompassed three primary stages: experimental and data preparation, RF model establishment and model validation, and model prediction. We initially investigated the OP and EPFRs concentrations in nine typical cities suffering from severe SDS in China. We previously found that the meteorological parameters and PM concentrations were factors determining the occurrence of EPFRs[34,35]. Therefore, before model development, the Boruta algorithm was used to pre-screen model parameters, including meteorological factors, air pollution indicators, and characteristics of the PM samples, such as the particle type (TYPE). Irrelevant variables were eliminated. This algorithm reduces the misleading effects of random fluctuations and correlations by introducing randomness to the system and deriving results from an ensemble of randomized samples. The selected variables, including meteorological factors [surface pressure (P_0), temperature, relative humidity (RH), visibility (VV), precipitation (RRR), wind speed, and maximum wind speed (ff3)]; and air quality data [fine particulate matter ($PM_{2.5}$), air quality index (AQI), inhalable particulate matter (PM_{10}), SO_2, O_3, CO and NO_2], had significantly affected the occurrence of EPFRs during SDS periods (Supplementary Fig. 1). Within the developed model (Supplementary Fig. 1), air quality data, specifically $PM_{2.5}$ and AQI were the most significant variables for EPFRs occurrences during SDS periods. Meteorological factors, such as P_0, temperature, and RH, also exhibited high importance. Furthermore, we filtered and validated the model's accuracy ($R^2 = 0.95$) using 10-fold cross validation and ultimately arrived at the optimum model (Supplementary Fig. 2). We then conducted a sensitivity analysis to further explore the model's performance (Supplementary Fig. 3), which varied with the number of variables tried at each split (mtry) and the number of trees (ntree). The RF model exhibited excellent predictive capabilities when the optimum values for ntree and mtry were set to 1100 and 15, respectively. Details for the RF modeling and 10-fold cross validation are provided in the Supplementary Results. We predicted the EPFRs concentrations at 1735 sites in China (Supplementary Fig. 4) during the SDS periods using the experimentally measured data and the established RF model. The linear regression results ($R^2_{Testing} = 0.88$, $R^2_{Training/Validation} = 0.96$) of the measured and predicted EPFRs concentrations indicated the model had excellent predictive performance (Fig. 2A, B). We also used a similar RF model to select significant variables for the OP and to precisely predict the OP concentrations (Fig. 2C, D) at 1735 sites in China (Supplementary Fig. 4) during the SDS periods. Details for use of the RF model for the OP are given in the Supplementary Results.

Levels and geospatial distribution of EPFRs and the OP during SDS periods
The concentrations and spatial distributions of EPFRs in total suspended PM (TSP) and $PM_{2.5}$ during the SDS periods in mainland China are shown in Fig. 3A, B, respectively. During the SDS periods, Inner Mongolia and Shanxi Province in North China and Yunnan and Guiyang provinces in South China had highest EPFRs concentrations for TSP and $PM_{2.5}$. The anthropogenic activity, natural activity, and migration process of dust PM from areas with high levels of air pollution may contribute to the high concentrations of EPFRs[24,26]. Additionally, the EPFRs on atmospheric PM from the northern region exhibited a diffusion pattern radiating from the northern boundary inland, while EPFRs from the southwestern region displayed a diffusion pattern radiating from the southwest boundary inland. Similar distribution characteristics were also observed for the OP of atmospheric PM (Fig. 3C). There were also high OP concentrations in areas such as the Yangtze River Delta, which is an area with extensive anthropogenic activity (e.g., residential biomass burning and vehicular emissions)[19]. These OP concentrations were comparable to or even higher than those in the dust-prone areas. Therefore, EPFRs were predominantly influenced by the dust distributions, while the OP was affected by both the dust distribution and anthropogenic activity during the SDS period. There were strong positive correlations between the atmospheric EPFRs, $PM_{2.5}$, AQI, and PM_{10} (Supplementary Fig. 5). EPFRs were
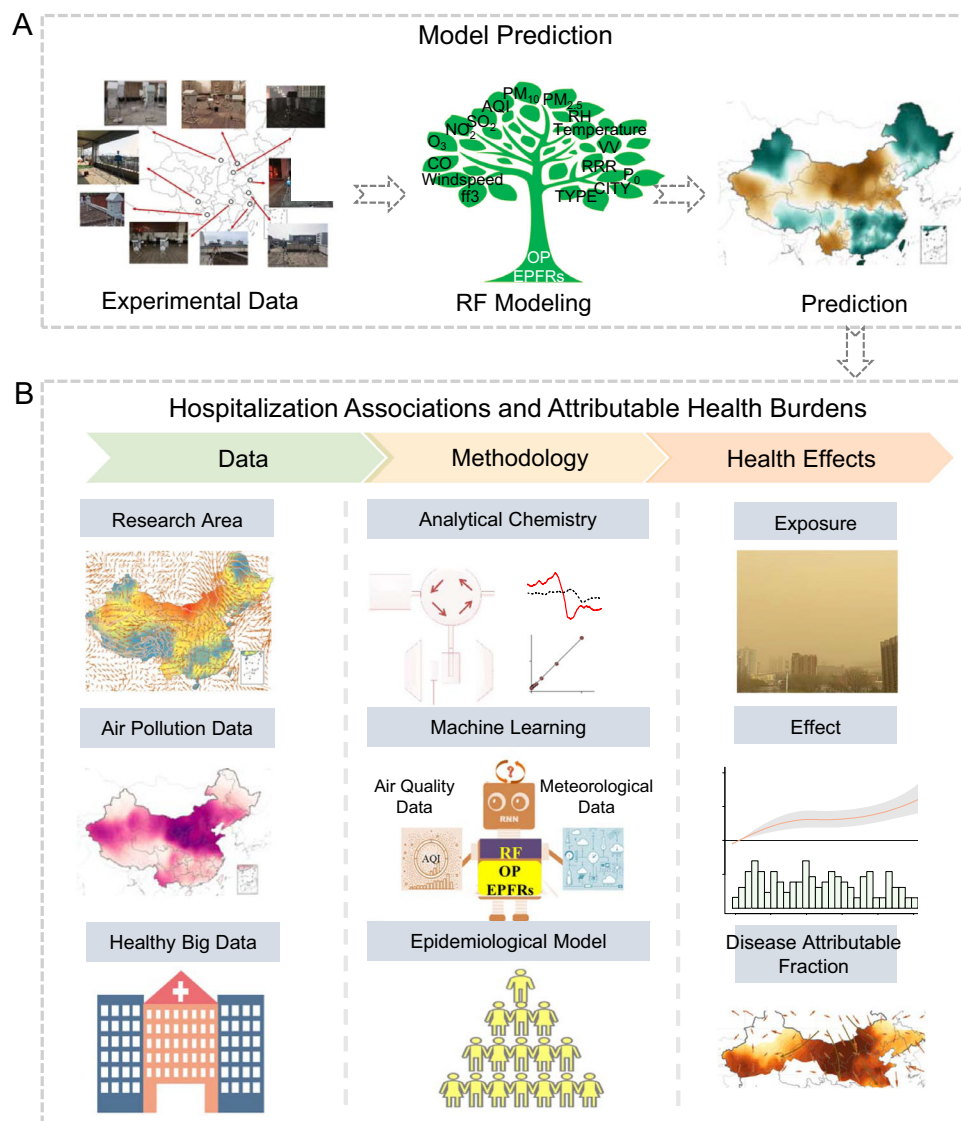
Fig. 1 | Modeling framework and overall strategy. A Flowchart of random forest (RF) modeling for the oxidative potential (OP) and environmentally persistent free radicals (EPFRs) concentrations predictions. **B** Flowchart of health risk assessment. The photos were taken on-site by the authors. The cartoon schematics were all drawn by the authors themselves. The maps were drawn based on the vector data from the National Platform for Common GeoSpatial Information Services (https://www.tianditu.gov.cn/) and Resource and Environmental Science Data Platform (https://www.resdc.cn/).

attached to and stabilized on fine particles[22,24,26,36]. Therefore, the EPFRs and fine particles will share the same transport trails. We used Hybrid Single Particle Lagrangian Integrated Trajectory (HYSPLIT) back trajectory to analyze the transport trail of dust particles (Supplementary Fig. 6). This analysis showed that the sources of sand and dust particles in the northern and southern regions were different. In northern regions, sand and dust particles originated from Mongolia. In southern regions, sand and dust particles were from the Indochina Peninsula and the Indian Peninsula. The concentrations of EPFRs on PM during the SDS periods were ~10 times those on PM during the non-SDS periods (Supplementary Fig. 7). An obvious increase in the OP of the PM was also observed during the SDS periods, with the SDS value approximately three times that during the non-SDS periods (Supplementary Fig. 8). Additionally, when a SDS passed through a city, it carried PM generated by urban activities, including aerosols such as automobile exhaust and industrial stack gas with high EPFRs concentrations[22,24,37] and OP[19,38]. The spatial distribution of PM_{10} and $PM_{2.5}$ (Supplementary Fig. 9 and Supplementary Fig. 10) also supported the geospatial distributions of EPFRs and the OP found in this study. Therefore, the transport trails of sand and dust particles could explain the distribution characteristics of EPFRs and the OP in China (Supplementary Fig. 6).

Link between the OP/EPFRs and hospitalizations
Between 2015 and 2022, more than 20 SDS events occurred in Beijing, China[2,39]. The average PM_{10} concentration in North China in 2021 showed a 39% increase compared with that in 2015–2020[2]. The fine particles and their EPFRs and OP might jointly induce adverse human health effects. During 2015–2022, a total of 855,869 hospitalizations occurred during the SDS periods, including 120,297 hospitalizations on identified SDS event days in Beijing (Table 1). There were 23,287 cases of influenza and pneumonia, which accounted for most respiratory diseases (29.85%), and 58,931 cases of cerebrovascular disease, which accounted for most circulatory diseases (36.82%).

To assess the impact of SDS events on a range of diseases at lag day 0, we analyzed the linear relationship of hospitalizations with the OP and EPFRs and $PM_{2.5}$ concentrations of dust particles (Fig. 4). There were significant correlations between the OP and EPFRs
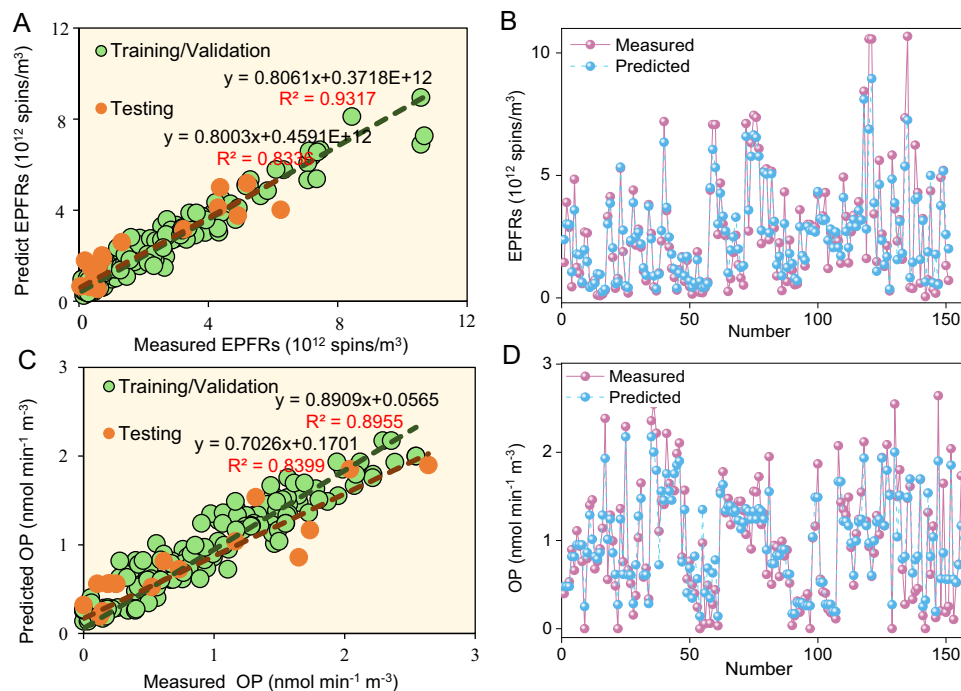
Fig. 2 | Comparison between modeled and measured concentrations. A, B Comparison between the modeled and measured environmentally persistent free radicals (EPFRs) concentrations. **C, D** Comparison between the modeled and measured oxidative potential (OP) concentrations. Source data are provided as a Source Data file.

concentrations and multiple diseases. The RR differed significantly from one ($P < 0.05$, blue points in Fig. 4) for 88% of the investigated diseases under EPFRs exposure, 84% of the investigated diseases under OP exposure, and 64% of the investigated diseases under $PM_{2.5}$ exposure (Fig. 4, Supplementary Table 1 and Supplementary Table 2). These results show that the OP and EPFRs concentrations of $PM_{2.5}$ are more sensitive than the $PM_{2.5}$ itself for health risk assessment of SDS.

Figure 4A shows that a 0.2 nmol/min/m^3 increase in the OP was associated with a 2.08% (95% CI: 1.13%, 3.04%) elevated relative risk (RR) of respiratory disease during the SDS periods. Similarly, each 0.2 nmol/min/m^3 increase in the OP was associated with a 3.52% (95% CI: 2.13%, 4.92%) increase in the RR of circulatory disease. Furthermore, short-term OP exposure during the SDS periods was significantly associated with heightened hospitalization risks for various diseases, including hypertensive disease, ischemic heart disease, acute ischemic heart disease, diseases of the arteries, arterioles, and capillaries, other forms of heart disease, diseases of the veins, lymphatic vessels, and lymph nodes (not otherwise specified), cerebrovascular diseases, influenza and pneumonia, pneumonia, ischemic stroke, other diseases of the upper respiratory tract, myocardial infarction, acute myocardial infarction, chronic lower respiratory disease, other chronic obstructive pulmonary diseases, and chronic obstructive pulmonary disease (Fig. 4A). Among all the sub-causes of circulatory and respiratory diseases, hypertensive diseases, influenza, and pneumonia exhibited the highest increased risks. Specifically, a 0.2 nmol/min/m^3 increase in the OP concentration was associated with an increased risk of 4.32% (95% CI: 2.10%, 6.59%) for hypertensive diseases and of 2.78% (95% CI: 1.43%, 4.15%) for influenza and pneumonia.

There were also significant associations between the EPFRs concentrations and various diseases (Fig. 4B, C). Each 10^{12} spins/m^3 increase in EPFRs on TSP was associated with 2.02% (95% CI: 1.01%, 4.08%) and 3.05% (95% CI: 1.01%, 4.08%) increases in respiratory disease and circulatory disease, respectively. By comparison, each 10^{12} spins/m^3 increase in EPFRs on $PM_{2.5}$ resulted in an increase in the adverse effects on respiratory (3.05%; 95% CI: 1.01%, 5.13%) and circulatory (4.08%; 95% CI: 2.12%, 6.18%) diseases. These results suggest there are more pronounced health risks caused by EPFRs on fine

particles than EPFRs on TSP. Additionally, short-term exposure to EPFRs was significantly associated with increased hospitalization risks for various diseases, including ischemic heart disease, diseases of the veins, lymphatic vessels, and lymph nodes (not otherwise specified), other forms of heart disease, hypertensive disease, chronic obstructive pulmonary disease, chronic lower respiratory disease, other diseases of the upper respiratory tract, other chronic obstructive pulmonary diseases, cerebrovascular diseases, ischemic stroke, myocardial infarction, influenza, and pneumonia. Among all the sub-causes of circulatory and respiratory diseases, acute ischemic heart disease and chronic obstructive pulmonary disease exhibited the largest increased risks. Specifically, every 10^{12} spins/m^3 increase in EPFRs was associated with 4.08% (95% CI: 2.02%, 5.13%) and 3.05% (95% CI: 1.01%, 5.12%) increases in acute ischemic heart disease and chronic obstructive pulmonary disease, respectively (Fig. 4A, B, and Supplementary Table 1).

Non-linear exposure–response relationships

Figure 5 shows the overall cumulative EPFRs or OP exposure–response curves for 16 districts in Beijing from 2015 to 2022. The thresholds for EPFRs and OP exposure levels for the minimum effects of all-cause hospitalization were obtained from the exposure–response curves (Fig. 5A, B), and were 10^{12} spins/m^3 and 0.3 nmol/min/m^3, respectively. These lowest adverse effect levels of EPFRs and the OP were comparable to those observed on clean days (Supplementary Fig. 11), which was evidence of the model accuracy. The exposure–response non-linear curves showed that the all-cause hospitalization risks increased with the OP or EPFRs concentration in a supralinear trend (Fig. 5). These results agreed with the results of the linear models showing positive correlations of EPFRs or OP with hospitalization (Fig. 5A, B).

Attributable health burdens

According to the EPFRs or OP exposure–response curves (Fig. 5A, B), we estimated the fraction of all-cause hospitalizations in dust-prone cities in China during the SDS periods in 2021 that could be attributed to OP and EPFRs exposure. The average attributable fractions for the OP and EPFRs were 20.47% (95% CI: 15.75%, 28.28%) and 27.26% (95% CI:
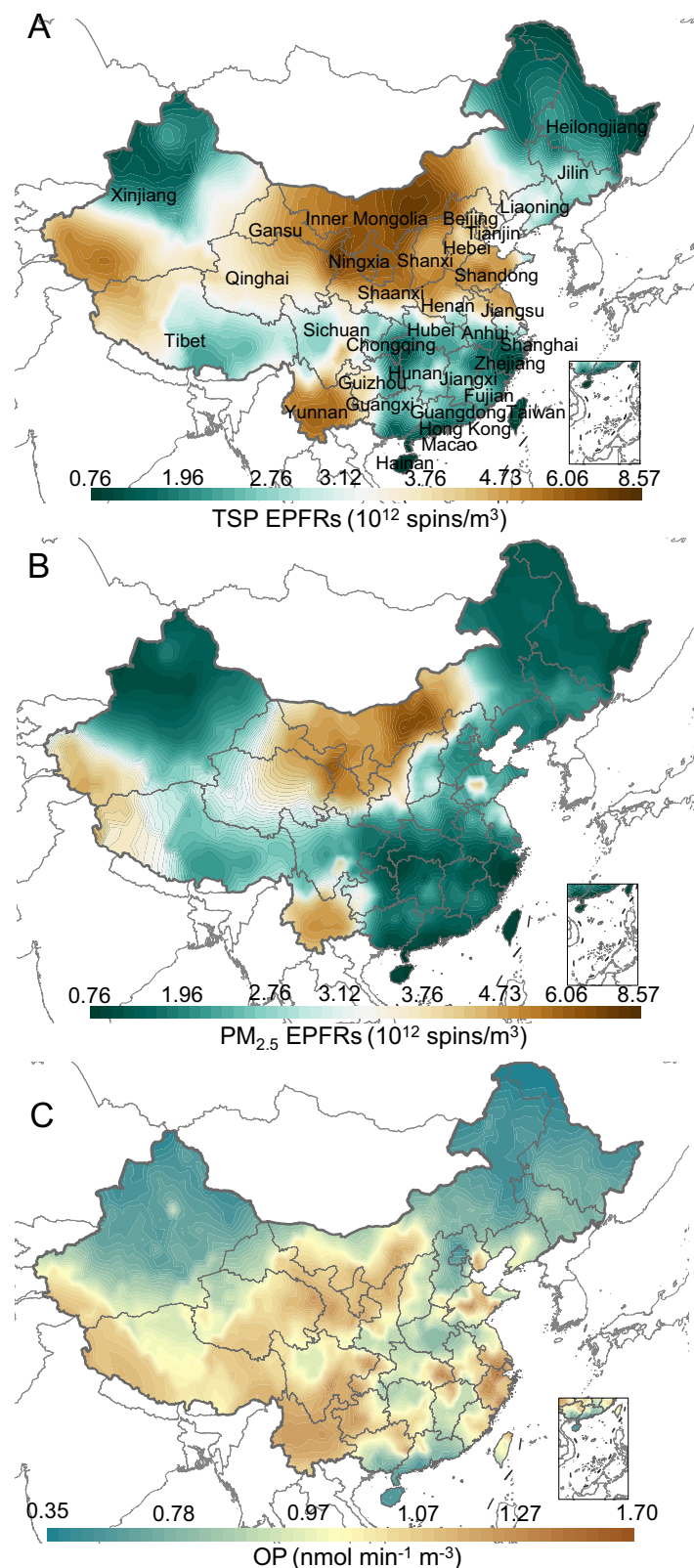
Fig. 3 | Spatial distribution of environmentally persistent free radicals (EPFRs) and oxidative potential (OP). A, **B** Spatial distribution of EPFRs in atmospheric particulate matter (PM) of different sizes during a dust storm in China (from 22:00 on March 27, 2021, to 24:00 on March 30, 2021). **C** Spatial distribution and levels of OP of atmospheric PM during a dust storm in China (from 22:00 on March 27, 2021, to 24:00 on March 30, 2021). $PM_{2.5}$: fine particulate matter of diameter lower than 2.5 um; TSP: total suspended particulate matter. The maps were drawn based on the vector data from the National Platform for Common GeoSpatial Information Services (https://www.tianditu.gov.cn/) and Resource and Environmental Science Data Platform (https://www.resdc.cn/). Source data are provided as a Source Data file.

Table 1 | Summary of statistics for daily hospitalizations in Beijing during SDS periods from 2015 to 2022

ICD-10	Cause of hospitalization	Total hospitalizations during the SDS periods	Mean daily hospitalizations during the SDS periods	Total hospitalizations on the SDS event days
A00-Z99	All-cause	855869	5468	120297
A00-R99	Non-accidental	696093	4445	97784
J00-J99	Diseases of the respiratory system	78024	482	10601
J09-J18	Influenza and Pneumonia	23287	136	2996
J12-J18	Pneumonia	22958	135	2967
J20-J22	Other acute lower respiratory infections	5461	33	717
J20	Acute bronchitis	5239	31	692
J30-J39	Other diseases of upper respiratory tract	7494	48	1061
J40-J47	Chronic lower respiratory disease	18124	122	2689
J41-J44	Chronic obstructive pulmonary disease	13246	91	2007
J44	Other chronic obstructive pulmonary disease	11665	81	1785
J98	Other respiratory distress syndromes	12560	75	1660
I00-I99	Diseases of the circulatory system	160058	1030	22649
I10-I15	Hypertensive diseases	10032	66	1454
I20-25	Ischemic heart diseases	52147	346	7617
I21-I22	Acute myocardial infarction	10086	66	1447
I21-I23	Myocardial infarction	10094	66	1448
I20-I22, I24	Acute ischemic heart disease	43933	292	6413
I25	Chronic ischemic heart disease	8206	55	1203
I30-I52	Other forms of heart disease	20024	135	2974
I60-I61	Hemorrhagic stroke	4631	30	665
I60-I63	Ischemic stroke	36499	229	5031
I60-I69	Cerebrovascular diseases	58931	376	8262
I70-I79	Diseases of arteries, arterioles, and capillaries	3662	23	498
I80-I89	Diseases of veins, lymphatic vessels, and lymph nodes, not elsewhere classified	12568	78	1718

20.12%, 33.77%), respectively. The spatial distribution of the OP and EPFRs attributable health burdens during the SDS periods throughout dust-prone areas of China were plotted (Fig. 5C, Fig. 5D, and Supplementary Fig. 12). The fractions of hospitalizations attributable to EPFRs were highest in regions with mass loads of sand and dust, including Inner Mongolia, Shaanxi, Shanxi, Gansu, and Hebei in North China (35.75%, 95% CI: 27.47%, 43.13%) and Yunnan provinces in South China (34.27%, 95% CI: 26.43%, 41.27%). Interior regions of China had a lower fraction of hospitalizations attributable to EPFRs at 24.81% (95% CI: 17.50%, 31.57%). As a result of differed exposure–response curves of OP and EPFRs, the spatial distribution of the OP attributable health burden was different with that of EPFRs. The fractions of all-cause hospitalization attributed to OP exposure were highest (22.34%; 95% CI: 15.82%, 28.37%) in regions with less sand and dust in East China, followed by regions with mass loads of sand and dust in Northeast China.

Discussion

In this study, we mapped the spatial distributions and trajectories of atmospheric OP and EPFRs at 1735 sites on a national scale during SDS periods in 2021 using machine learning algorithms. These two PM metrics can both contribute to oxidative stress[16,18,19,40,41]. However, their health risks are largely unknown. Previous studies on sand- and dust-induced health risks have mainly focused on PM fractions. The health burden of critical PM metrics, such as emerging EPFRs and the OP, has not been clarified. Here, by integrating epidemiological data encompassing 855,869 hospitalizations during SDS periods from 2015 to 2022 in Beijing, China, we investigated the cause-specific hospitalization risks associated with short-term exposure to the PM OP or EPFRs. From the

perspective of the disease spectrum and all-cause burden analysis, we clarified the exposure–response relationship between the OP, EPFRs, PM, and multiple diseases during the SDS periods and their corresponding attributable health burdens. Therefore, this study quantitatively evaluated the health burden of PM metrics during SDS periods.

Even though sand and dust had considerable concentrations of EPFRs, fine particles, and OP (Fig. 3 and Supplementary Fig. 9) and they shared the same transport trails throughout China (Supplementary Fig. 6), their correlation with and sensitivity to assess health risks were different (Fig. 4). Both the OP and EPFRs were sensitive for risk assessment of the total 855,869 hospitalizations during the dust storm period, and their sensitivities were even higher than that of $PM_{2.5}$ concentrations. These results imply that the OP and EPFRs on PM should be the focus when evaluating the health risks of SDS.

Short-term OP exposure was linked with both respiratory and circulatory diseases. The effects of the OP on circulatory (3.52; 95% CI: 2.13, 4.92) and respiratory diseases (2.08; 95% CI: 1.13, 3.04) with each 0.2 nmol/min/m³ increase were statistically significant ($P < 0.05$), especially for the risks on circulatory diseases. For cause-specific circulatory hospitalizations, we observed high risks for hypertensive diseases (4.32; 95% CI: 2.10%, 6.59%) with each 0.2 nmol/min/m³ increase in OP exposure. Previous studies have reported that oxidative stress can damage the vascular endothelium, increase platelet activity, and promote thrombus formation by enhancing coagulation[17,42], which may explain the association of the OP with circulatory disease found in this study. For cause-specific respiratory hospitalizations, pneumonia hospitalization associated with the OP increased largely during the SDS periods. This result is in accordance with previous studies[18,20] and
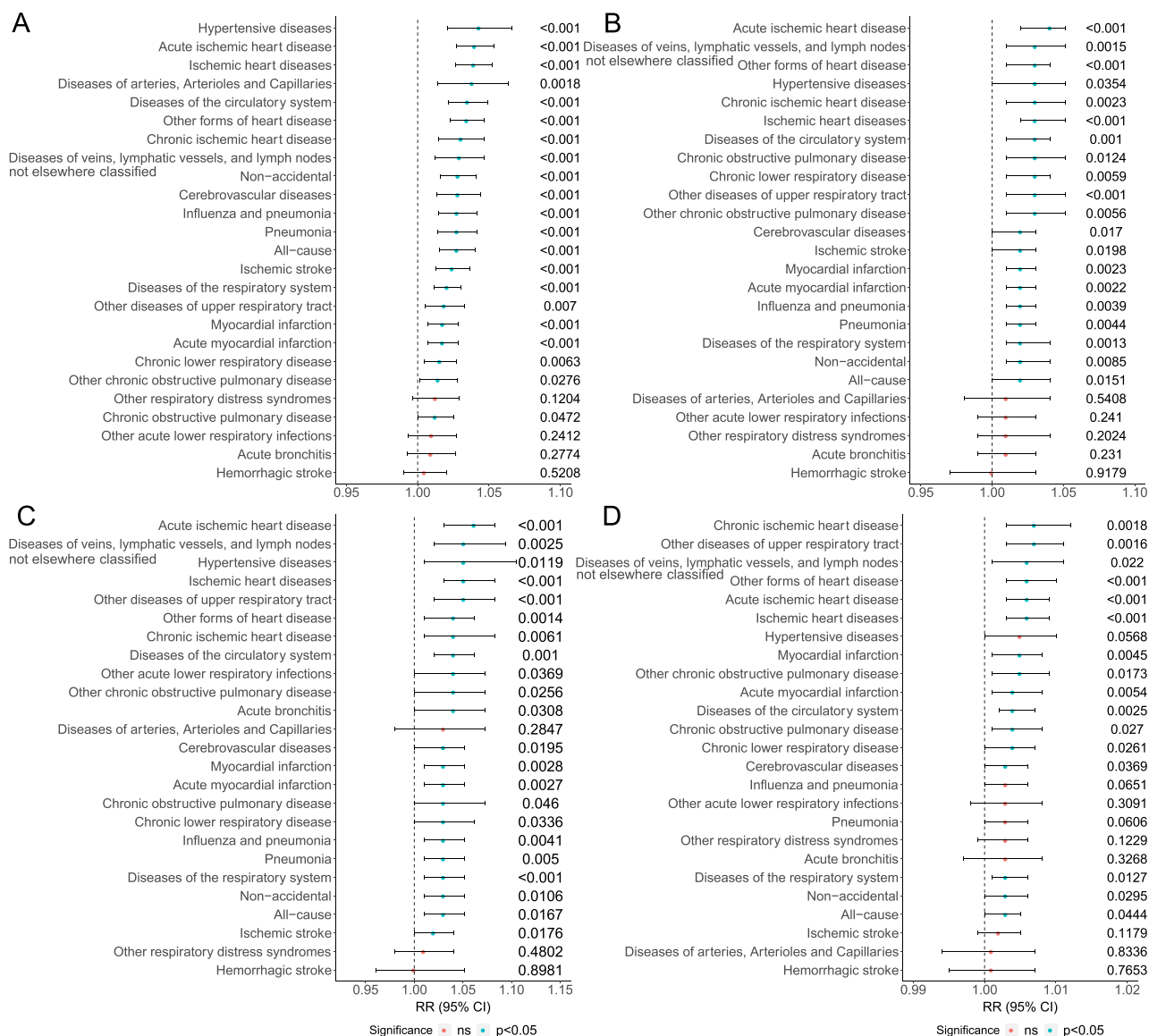
Fig. 4 | Pooled relative risks (RR) of all-cause, cardiovascular, and respiratory hospitalizations associated with sandstorm event-related environmentally persistent free radicals (EPFRs), oxidative potential (OP), and fine particulate matter (PM$_{2.5}$). A RR for a 0.2 nmol min/m^3 increase in OP of particulate matter (PM). **B** RR for a 10^{12} spins/m^3 increase in EPFRs on total suspended PM (TSP). **(C)** RR for a 10^{12} spins/m^3 increase in EPFRs on PM$_{2.5}$. **D** RR for a 10 μg/m^3 increase in PM$_{2.5}$.

The estimates are pooled for the study area ($n = 16$), incorporating a total of 855,869 hospitalizations. The black error bar represents a 95% confidence interval (CI), with the center of the error bar indicating the point estimate of the RR. P-values are evaluated based on Wald tests. $P < 0.05$ is considered statistically significant, while NS indicates that the result is not significant. The corresponding P-value is presented on the right. Source data are provided as a Source Data file.

indicates that pneumonia patients could be highly vulnerable to the adverse effects of the OP during SDS periods.

EPFRs are emerging contaminants on atmospheric PM that can enter the human body along with PM and induce formation of ROS[22,23,38,43]. Some in vitro experiments have been conducted on the adverse health effects of EPFRs[44-50] and found some biological mechanisms that seem to support our findings. In this study, we found that each 10^{12} spins/m^3 increase in EPFRs was significantly associated with circulatory (3.05%; 95% CI: 1.01%, 4.08%) and respiratory (2.02%; 95% CI: 1.01%, 4.08%) diseases during the SDS periods. For cause-specific circulatory diseases, exposure to EPFRs was consistently associated with hospitalizations from several heart diseases, with acute ischemic heart disease having the highest risk (4.08% [95% CI: 2.02%, 5.12%] increase for each 10^{12} spins/m^3 increase in EPFRs). Previous in vitro cell experiments have found that EPFRs can cause apoptosis in HL-1 cardiomyocytes[47,50], which could explain the association between

EPFRs exposure and heart disease observed in this study. PM is widely recognized as an important pathogenic substance when evaluating air pollution-related health risks[14,16,17,51]. In this study, each 10 μg/m^3 increase in PM$_{2.5}$ was associated with 3.01% (95% CI: 1.01%, 6.02%) and 4.01% (95% CI: 2.00%, 7.02%) increases in respiratory and circulatory diseases, respectively. Therefore, the OP, EPFRs and PM, especially the OP and EPFRs, all had significant adverse effects on heart disease and hypertension-related diseases (Fig. 4). Because both the OP and EPFRs can result in oxidative stress[18,40,41,47], they can damage the cardiovascular system and induce related disorders.

The overall cumulative EPFRs or OP exposure-response curves for 16 districts in Beijing showed a supralinear trend. According to the EPFRs and OP exposure-response curves, the fraction of all-cause hospitalizations in dust-prone areas of China during the SDS periods in 2021 that could be attributed to OP and EPFRs exposure were estimated (Fig. 5). We found that OP and EPFRs exposure was a
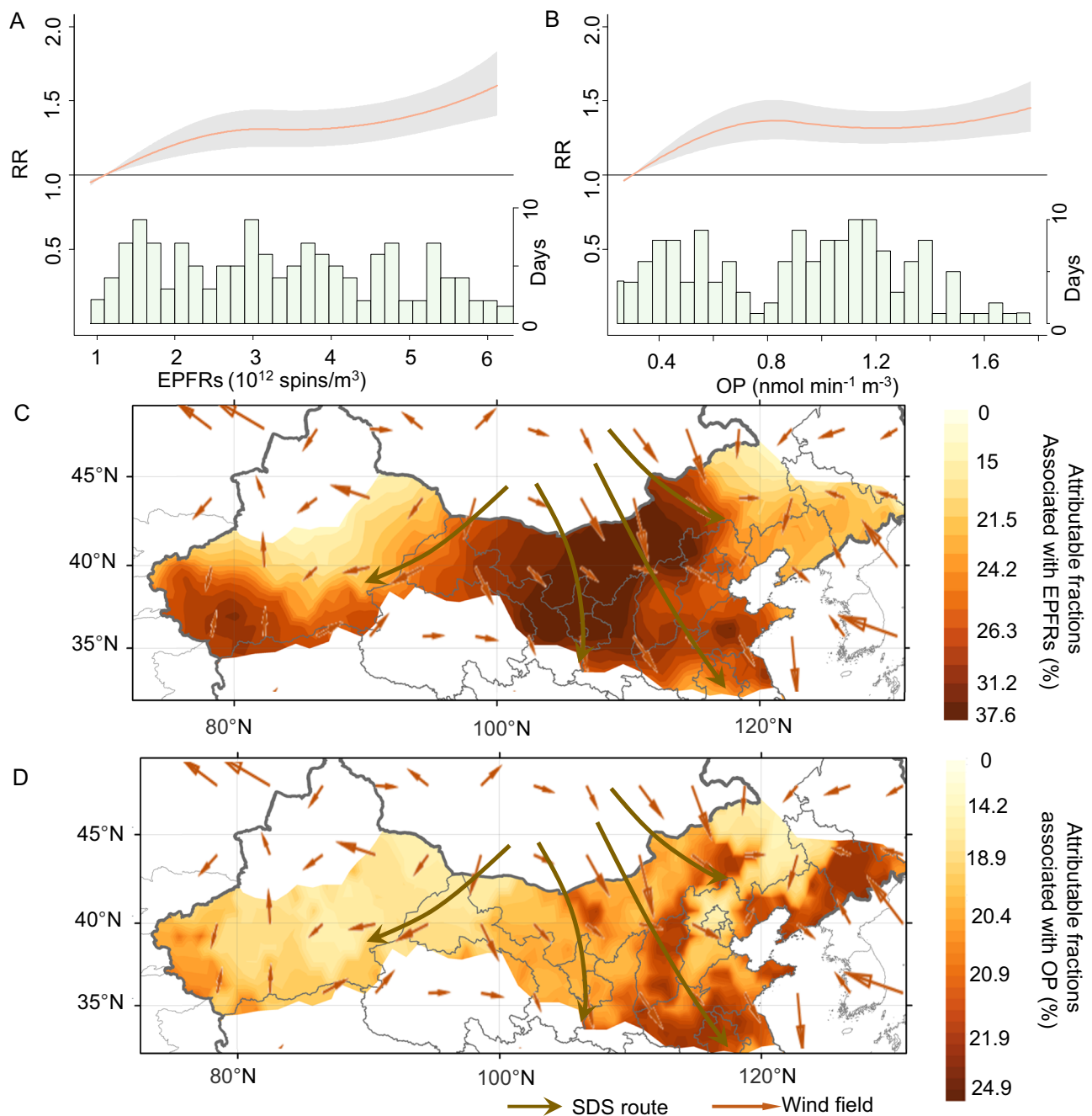
Fig. 5 | Nonlinear associations and attributable fractions of hospitalization linked to environmentally persistent free radicals (EPFRs) and oxidative potential (OP). Estimated nonlinear association between all-cause hospitalization and (**A**) EPFRs and (**B**) OP exposure, respectively. Attributable fractions associated with short-term sand and dust storms (SDS)-related (**C**) EPFRs and (**D**) OP during SDS events in dust-prone areas of North China (from 22:00 on March 27, 2021, to 24:00 on March 30, 2021). RR: relative risks. The partial maps were drawn based on the vector data from the National Platform for Common GeoSpatial Information Services (https://www.tianditu.gov.cn/) and Resource and Environmental Science Data Platform (https://www.resdc.cn/). Source data are provided as a Source Data file.

considerable risk factor and could pose health burdens to all-cause hospitalization. During the SDS periods, both the OP and EPFRs contributed to the health burdens in regions of mass loads of sand and dust. By contrast, in regions with low sand and dust but high anthropogenic activity, OP was the dominant contributor to the health burden. The EPFRs were strongly positively correlated with the sand and dust particles, and the OP was closely related to CO and NO_2 (Supplementary Fig. 1 and Supplementary Fig. 5). These results are in accordance with previous studies[19]. When the *RR* values were combined with the exposure–response curves, the attributable health burdens of EPFRs were highest in regions with mass loads of sand and

dust. The attributable health burdens of the OP were highest in densely populated areas.

This study has several strengths. It is the first study to assess the association between hospitalizations for multiple diseases and PM metrics, including the OP and EPFRs, which are critical factors that induce oxidative stress. When evaluating the sand and dust health risks, we found that OP and EPFRs were even more sensitive than PM for health risk assessments during SDS. Furthermore, this was a long-term epidemiological study (2015–2022) on the basis of the valuable OP and EPFRs concentrations on $PM_{2.5}$ and TSP surfaces at 1735 sites in China. The large number of sites of EPFRs and OP concentrations and

the long period of epidemiology study provide accurate analysis of the exposure–response associations. Finally, we found that the attributable fraction of EPFRs and OP exposure to all-cause hospitalization presented spatial variations in dust-prone areas of China during SDS periods. These results are insightful for effective sand and dust risk prevention in dust-prone countries.

A limitation of this study is that we mainly focused on the OP and EPFRs exposure–response associations during severe SDS events, which had maximum PM_{10} concentrations reaching up to 1000 µg/m^3. The health risks of backflow SDS with PM_{10} concentrations <1000 µg/m^3 were not evaluated. The potential health risks of backflowing sand and dust may be even higher than those of the initial sand and dust[52]. Because sandstorms pass through multiple regions, the sand and dust PM will mix with anthropogenic PM, which makes the composition of backflowing PM more complex than the original SDS PM. The health risks of backflowing sand and dust should be investigated in future studies. Another limitation of this study was that the specific diseases focused on were respiratory and circulatory disease that are correlated with PM pollution[14,17,51]. Further research should be conducted to explore disease subclasses that were found to be sensitive to EPFRs and OP exposure from SDS in this study.

SDS are severe and common air pollution events worldwide and have become a priority for research within the global community. The World Health Organization (https://iris.who.int/handle/10665/345329) has suggested global air quality guidelines to address the health risks of SDS[53], but there is insufficient knowledge for quantitative and qualitative health risk assessments of SDS. Exploring the health effects of SDS-related pollutants can provide evidence to formulate uniform air quality guidelines and facilitate the achievement of sustainable development goals (https://www.who.int/europe/about-us/our-work/sustainable-development-goals).

In this study, we explored the association between hospitalizations for multiple diseases and the OP and emerging EPFRs content of PM during SDS periods in China. The OP and EPFRs are critical factors that induce oxidative stress. During SDS periods, the OP and EPFRs were more sensitive than PM for disease risk assessments. Short-term exposure to OP and EPFRs had significant adverse effects, especially on heart disease and hypertension-related disease. The OP and EPFRs can create an all-cause hospitalization health burden during SDS periods. We found that the effects of the OP and EPFRs differed with the region. The attributable health burdens of the OP were highest in densely populated areas, while EPFRs mainly affected regions with mass loads of sand and dust. Our results show that these two factors are crucial for evaluating SDS health risks and the spatial characteristics of health burdens, which could be used to develop effective sand and dust risk prevention measures in dust-prone countries.

Methods
This study complies with all relevant ethical regulations and was approved by the Research Center for Eco-Environmental Sciences, Chinese Academy of Sciences.

Atmospheric PM sampling and trajectory simulation
The sampled cities were sources, transit locations, and sinks for sand and dust during the storms (Supplementary Fig. 13). The wind direction was considered for the distribution of sampling points. The number of sampling points upwind and downwind were set according to the city size, topography, and the severity of the dust storm. Variations in pollution levels before, during, and after the dust storms were evaluated. PM of various sizes (TSP, PM_{10}, $PM_{2.5}$, and submicronic particulate matter [$PM_{1.0}$]) were simultaneously collected. The details for the sample collection methods are given in the Supplementary Methods. In total, 190 atmospheric PM samples were collected from nine cities (Beijing, Hohhot, Shijiazhuang, Qingdao, Wuhan, Yancheng, Hangzhou, Guiyang, and Chengdu) during the SDS period of 2021–2023.

The HYSPLIT model, which was established by the Air Resources Laboratory of the National Oceanic and Atmospheric Administration and the Australian meteorological service, was used in this study to simulate the trajectories and spatial distributions of individual types of PM in the air.

Quantification of the OP and EPFRs on PM during SDS periods
EPFRs on the surfaces of atmospheric PM of various sizes were analyzed by electron paramagnetic resonance spectroscopy (Bruker EMX Plus X-band, Billerica, MA, USA). The sample pretreatment methods and detection parameters (detailed in the Supplementary Methods) were developed with reference to previous studies[22,34,54]. Three replicates were measured for each sample (Supplementary Fig. 14).

The OP of PM of various sizes during the SDS periods were assessed using the dithiothreitol (DTT) assay, which is the most frequently used non-cellular approach to measure the OP[19,55,56]. In the DTT assay, redox-active species in PM can transfer electrons from DTT to oxygen, which generates superoxide radicals[57]. The OP of these species is quantitatively evaluated using the consumption rate of DTT. The DTT activity measurements in this study were conducted using established methods[38,55,58]. Details for the OP analysis are provided in the Supplementary Methods. The decay rate of DTT was calculated from the slope of the linear regression curve between the residual DTT and time. The calibration curve for DTT is shown in Supplementary Fig. 15. The absorbance intensity of DTT at 412 nm was directly proportional to its concentration. The blank-corrected OP of the dust PM was subtracted from the procedural blank filter (3.7 nM/min) to estimate the OP [nmol/min/m^3] of the atmospheric PM.

Air pollution and meteorological data collection
Hourly air quality data, including the AQI and the concentrations of conventional air pollutants (PM_{10}, $PM_{2.5}$, SO_2, NO_2, CO, and O_3), were obtained from China National Environmental Monitoring Centre and National Urban Air Quality Real-Time Distribution Platform. Meteorological data, including P_0, temperature, RH, visibility, precipitation, average wind speed, and maximum wind speed, were obtained from the National Climatic Data Center of the United States. We extracted meteorological data and the corresponding air quality data from each station according to their geographical coordinates. Air quality data and meteorological data were obtained for 1735 sites in China (Supplementary Fig. 4).

Hospital admission data collection
Beijing has frequent SDS. In this study, we collected daily hospital admission data from 2015–2022 for all districts in Beijing from the Beijing Municipal Health Big Data and Policy Research Center. We analyzed the link between hospitalizations and EPFRs[40,41,47,49,50] and the OP[16,18,21]. This study treated the hospitalization cases for specific diseases as a whole across all sexes and ages. The primary diagnosis was coded according to the International Classification of Diseases, Tenth revision (ICD-10). We analyzed 27 hospitalization outcomes, including hospitalizations from four broad category causes (all-cause, non-accidental, diseases of the respiratory system, and diseases of the circulatory system) and 23 specific causes (Table 1).

Modeling of relationship between EPFRs/the OP and hospitalizations
We applied a two-stage strategy to analyze the associations between short-term EPFRs or OP exposure and hospitalizations during SDS periods[51,59,60]. In the first stage, we conducted region-specific time-series analyses using a quasi-Poisson generalized linear model with distributed lag terms[60].

$$\log E(Y_t) = \beta Z_t + ns(\text{Time}_t, df) + ns(\text{Temp}_t, df) \tag{1}$$

The model incorporated an indicator for the day of the week to account for within-week variations, and a natural spline function with three degrees of freedom per year to control for long-term trends and seasonal variations. The air temperature was modeled using a distributed lag nonlinear model, which consisted of a quadratic B-spline with three knots placed at the 0th, 50th, and 100th percentiles for the exposure–response relationship and a step function with a strata lag of 0 days for the lag–response relationship. In the main model, the exposure–response relationship was assumed to be linear with a lag of 0 days[13]. We also modeled the non-linear exposure-response curves and more complex associations with EPFRs/the OP using a distributed lag non-linear model. Non-linear exposure-response association and the additional lag response association were combined in this model. Specifically, we modeled the exposure-response curve with a quadratic B-spline with three knots placed at the 0th, 50th, and 100th percentiles of location-specific EPFRs/the OP distributions.

In the second stage, we combined the specific estimates using a mvmeta-analysis fitted with restricted maximum likelihood. The second stage estimate represents the pooled effect for the study area, while district- and study area-specific estimates were derived as best linear unbiased predictions at the corresponding aggregation level. The best linear unbiased predictions used information from pooled associations to make more accurate location-specific estimates by borrowing information from the entire sample. All estimates are reported as the RR for a 10^{12} spins/m³ increase in EPFRs and a 0.2 nmol/min/m³ increase in the OP, with corresponding 95% confidence intervals (CIs). CIs were calculated using the standard error of the quasi-Poisson regression under the 95% confidence level[13,59–61].

Attributable health burdens

We initially explored potential nonlinear exposure–response shapes and more complex lag structures using a quintic polynomial model, and then using a distributed lag model with a natural spline. Polynomial parameterization was used to mitigate the sensitivity of the estimates to varying concentration ranges. The polynomial terms were not limited to a specific region but extended across the entire variable range. In both extensions, specific estimates of the multiparameter associations were pooled using a mvmeta-analysis[60,61].

To assess potential changes in risk over time, we subset the specific data and performed the first-stage model in multiple subperiods by splitting the time series into intervals. Specific estimates were pooled in a longitudinal multilevel meta-regression using time (defined as the midyear of each subperiod) as a continuous fixed-effect term[60]. Using the model, we computed additional hospitalizations associated with short-term exposure to OP and EPFRs using a previously described method[59,60]. The RR within lag 0 was used to compute the excess daily hospitalizations, adopting a forward perspective and using the standard formula β for continuous exposure. The following equation was used to calculate the RR for hospitalizations associated with exposure to OP and EPFRs:

$$RR = [\exp(C_a \times \beta)] \tag{2}$$

where β is the coefficient of the estimated effect; and C_a are the unit increases in concentration for the OP and EPFRs, which were assigned as 0.2 nmol/min/m³ and 10^{12} spins/m³, respectively.

To quantify the hospitalization burden attributable to the OP and EPFRs, we used the following equation for a standard risk assessment:

$$AF_{s,t} = 1 - \frac{1}{f(C_{s,t})} \tag{3}$$

where s is space, t is time; $C_{s,t}$ is the OP or EPFRs concentration that exceeds the OP and EPFRs concentration on a clean day, which was taken as the minimum risk exposure level; and f is the non-linear

association between the OP or EPFRs, with hospitalizations estimated from the regression analyses.

Furthermore, we conducted a sensitivity analysis by modifying the modeling choices and replacing all-cause hospitalization with non-accident hospitalization. We varied the lag day from 0 to 1 or 2 days for the OP and EPFRs. Additionally, we adjusted the degrees of freedom for meteorological variables (from 2 to 3, 4, or 5). Supplementary Table 1 and Supplementary Table 2 provide detailed results from the sensitivity analysis. All analyses were conducted using R programming language (version 4.2.2, R Core Team) using the *dlnm* and *mvmeta* packages.

Reporting summary

Further information on research design is available in the Nature Portfolio Reporting Summary linked to this article.

References

1. Penner, J. Three ways through the soot, sulfates and dust. *Nature* **570**, 158–159 (2019).
2. Yin, Z., Wan, Y., Zhang, Y. & Wang, H. Why super sandstorm 2021 in North China? *Natl Sci. Rev.* **9**, nwab165 (2021).
3. Rodriguez-Caballero, E. et al. Global cycling and climate effects of aeolian dust controlled by biological soil crusts. *Nat. Geosci.* **15**, 458 (2022).
4. WMO. *Sand and Dust Storm Warning Advisory and Assessment System.* https://library.wmo.int/records/item/57122-sand-and-dust-storm-warning-advisory-and-assessment-system (2020).
5. Jin, J. B. et al. Inverse modeling of the 2021 spring super dust storms in East Asia. *Atmos. Chem. Phys.* **22**, 6393–6410 (2022).
6. Liang, L. et al. Emission, transport, deposition, chemical and radiative impacts of mineral dust during severe dust storm periods in March 2021 over East Asia. *Sci. Total Environ.* **852**, 158459 (2022).
7. Arnold, C. Dust storms and human health: a call for more consistent, higher-quality studies. *Environ. Health Perspect.* **128**, 114001 (2020).
8. Schweitzer, M. D. et al. Lung health in era of climate change and dust storms. *Environ. Res.* **163**, 36–42 (2018).
9. Pan, X. C. & Liu, J. H. Study on health effects of dust storms (Asian Dusts) in China. *Epidemiology* **22**, S26–S27 (2011).
10. Kouis, P. et al. Mitigating the health effects of desert dust storms through exposure reduction approaches: the LIFE MEDEA Asthma study. *Eur. Respir. J.* **54**, PA2831 (2019).
11. Gross, J. E., Carlos, W. G., Dela Cruz, C. S., Harber, P. & Jamil, S. Sand and dust storms: acute exposure and threats to respiratory health. *Am. J. Respir. Crit. Care Med.* **198**, P13–P14 (2018).

12. Hashizume, M. et al. Health effects of Asian dust: a systematic review and meta-analysis. *Environ. Health Perspect.* **128**, 066001 (2020).

13. Zhang, C. et al. Mortality risks from a spectrum of causes associated with sand and dust storms in China. *Nat. Commun.* **14**, 6867 (2023).

14. Cohen, A. J. et al. Estimates and 25 year trends of the global burden of disease attributable to ambient air pollution: an analysis of data from the global burden of diseases study 2015. *Lancet* **389**, 1907–1918 (2017).

15. Jimenez, J. L. et al. Evolution of organic aerosols in the atmosphere. *Science* **326**, 1525–1529 (2009).

16. Kelly, F. J. & Sandstrom, T. Air pollution, oxidative stress, and allergic response. *Lancet* **363**, 95–96 (2004).

17. Brook, R. D. et al. Particulate matter air pollution and cardiovascular disease an update to the scientific statement from the American heart association. *Circulation* **121**, 2331–2378 (2010).

18. Bates, J. T. et al. Review of acellular assays of ambient particulate matter oxidative potential: methods and relationships with composition, sources, and health effects. *Environ. Sci. Technol.* **53**, 4003–4019 (2019).

19. Daellenbach, K. R. et al. Sources of particulate-matter air pollution and its oxidative potential in Europe. *Nature* **587**, 414–419 (2020).

20. Suri, R. et al. Exposure to welding fumes and lower airway infection with Streptococcus pneumoniae. *J. Allergy Clin. Immunol.* **137**, 527 (2016).

21. Abrams, J. Y. et al. Associations between ambient fine particulate oxidative potential and cardiorespiratory emergency department visits. *Environ. Health Perspect.* **125**, 107008 (2017).

22. Yang, L. et al. Highly elevated levels and particle-size distributions of environmentally persistent free radicals in haze-associated atmosphere. *Environ. Sci. Technol.* **51**, 7936–7944 (2017).

23. Gehling, W., Khachatryan, L. & Dellinger, B. Hydroxyl radical generation from environmentally persistent free radicals (EPFRs) in PM2.5. *Environ. Sci. Technol.* **48**, 4266–4272 (2014).

24. Vejerano, E. P., Rao, G. Y., Khachatryan, L., Cormier, S. A. & Lomnicki, S. Environmentally persistent free radicals: insights on a new class of pollutants. *Environ. Sci. Technol.* **52**, 2468–2481 (2018).

25. Qin, L. J. et al. Photoinduced formation of persistent free radicals, hydrogen radicals, and hydroxyl radicals from catechol on atmospheric particulate matter. *Iscience* **24**, 102193 (2021).

26. Sigmund, G. et al. Environmentally persistent free radicals are ubiquitous in wildfire charcoals and remain stable for years. *Commun. Earth Environ.* **2**, 68 (2021).

27. Liu, S., Liu, G., Yang, L., Li, D. & Zheng, M. Critical influences of metal compounds on the formation and stabilization of environmentally persistent free radicals. *Chem. Eng. J.* **427**, 131666 (2022).

28. Dellinger, B. et al. Formation and stabilization of persistent free radicals. *Proc. Combust. Inst.* **31**, 521–528 (2007).

29. dela Cruz, A. L., Gehling, W., Lomnicki, S., Cook, R. & Dellinger, B. Detection of environmentally persistent free radicals at a superfund wood treating site. *Environ. Sci. Technol.* **45**, 6356–6365 (2011).

30. Saravia, J., Lee, G. I., Lomnicki, S., Dellinger, B. & Cormier, S. A. Particulate matter containing environmentally persistent free radicals and adverse infant respiratory health effects: a review. *J. Biochem. Mol. Toxicol.* **27**, 56–68 (2013).

31. Balakrishna, S. et al. Environmentally persistent free radicals amplify ultrafine particle mediated cellular oxidative stress and cytotoxicity. *Part. Fibre Toxicol.* **6**, 11 (2009).

32. Dellinger, B. *Newly Detected Air Pollutant Mimics Damaging Effects of Cigarette Smoke.* https://www.chemeurope.com/en/news/85880/newly-detected-air-pollutant-mimics-damaging-effects-of-cigarette-smoke.html (2008).

33. Dellinger, B. et al. Role of free radicals in the toxicity of airborne fine particulate matter. *Chem. Res. Toxicol.* **14**, 1371–1377 (2001).

34. Xu, Y. et al. Assessment of personal exposure to environmentally persistent free radicals in airborne particulate matter. *J. Hazard. Mater.* **409**, 125014 (2020).

35. Xu, Y. et al. Risk evaluation of environmentally persistent free radicals in airborne particulate matter and influence of atmospheric factors. *Ecotoxicol. Environ. Saf.* **196**, 110571 (2020).

36. Chen, N. et al. The degradation of diethyl phthalate by reduced smectite clays and dissolved oxygen. *Chem. Eng. J.* **355**, 247–254 (2019).

37. Yang, L. et al. Pivotal roles of metal oxides in the formation of environmentally persistent free radicals. *Environ. Sci. Technol.* **51**, 12329–12336 (2017).

38. Hwang, B. et al. Environmentally persistent free radicals, reactive oxygen species generation, and oxidative potential of highway PM2.5. *ACS Earth Space Chem.* **5**, 1865–1875 (2021).

39. Song, L. *Yearbook of Meteorological Disasters in China.* https://www.scirp.org/reference/referencespapers?referenceid=2900940 (2022).

40. Balakrishna, S. et al. Environmentally persistent free radicals induce airway hyperresponsiveness in neonatal rat lungs. *Part. Fibre Toxicol.* **8**, 11 (2011).

41. Lee, G. I. et al. Exposure to combustion generated environmentally persistent free radicals enhances severity of influenza virus infection. *Part. Fibre Toxicol.* **11**, 57 (2014).

42. Piepoli, M. F. et al. 2016 European Guidelines on cardiovascular disease prevention in clinical practice. *Eur. Heart J.* **37**, 2315 (2016).

43. Khachatryan, L., Vejerano, E., Lomnicki, S. & Dellinger, B. Environmentally persistent free radicals (EPFRs). 1. Generation of reactive oxygen species in aqueous solutions. *Environ. Sci. Technol.* **45**, 8559–8566 (2011).

44. Bogdal, C. et al. Emissions of polychlorinated biphenyls, polychlorinated dibenzo-p-dioxins, and polychlorinated dibenzofurans during 2010 and 2011 in Zurich, Switzerland. *Environ. Sci. Technol.* **48**, 482–490 (2014).

45. Lemieux P. M., Lee C. W., Kilgroe J. D., Ryan J. V. Emissions of polychlorinated biphenyls from combustion sources. In *ACS Symposium Series* (2000).

46. Pirard, C. et al. Environmental and human impact of an old-timer incinerator in terms of dioxin and PCB level: a case study. *Environ. Sci. Technol.* **39**, 4721–4728 (2005).

47. Chuang, G. C., Xia, H., Mahne, S. E. & Varner, K. J. Environmentally persistent free radicals cause apoptosis in HL-1 cardiomyocytes. *Cardiovasc. Toxicol.* **17**, 140–149 (2017).

48. Fahmy, B. et al. In vitro and in vivo assessment of pulmonary risk associated with exposure to combustion generated fine particles. *Environ. Toxicol. Pharmacol.* **29**, 173–182 (2010).

49. Jaligama, S. et al. Regulatory T cells and IL10 suppress pulmonary host defense during early-life exposure to radical containing combustion derived ultrafine particulate matter. *Respir. Res.* **18**, 15 (2017).

50. Mahne, S. et al. Environmentally persistent free radicals decrease cardiac function and increase pulmonary artery pressure. *Am. J. Physiol. Heart Circ. Physiol.* **303**, H1135–H1142 (2012).

51. Dominici, F. et al. Fine particulate air pollution and hospital admission for cardiovascular and respiratory diseases. *JAMA* **295**, 1127–1134 (2006).

52. Lu, D. et al. Secondary aerosol formation during a special dust transport event: impacts from unusually enhanced ozone and dust backflows over the ocean. *Atmos. Chem. Phys.* **23**, 13853–13868 (2023).

53. WHO. *WHO Global Air Quality Guidelines: Particulate Matter (PM2.5 and PM10), Ozone, Nitrogen Dioxide, Sulfur Dioxide, and Carbon Monoxide.* https://iris.who.int/handle/10665/345329 (2021).

54. Arangio, A. M., Tong, H., Socorro, J., Pöschl, U. & Shiraiwa, M. Quantification of environmentally persistent free radicals and reactive oxygen species in atmospheric aerosol particles. *Atmos. Chem. Phys.* **16**, 13105–13119 (2016).

55. Charrier, J. G. & Anastasio, C. On dithiothreitol (DTT) as a measure of oxidative potential for ambient particles: evidence for the importance of soluble transition metals. *Atmos. Chem. Phys.* **12**, 9321–9333 (2012).

56. Charrier, J. G. et al. Oxidant production from source-oriented particulate matter – part 1: oxidative potential using the dithiothreitol (DTT) assay. *Atmos. Chem. Phys.* **15**, 2327–2340 (2015).

57. Kumagai, Y. et al. Oxidation of proximal protein sulfhydryls by phenanthraquinone, a component of diesel exhaust particles. *Chem. Res. Toxicol.* **15**, 483–489 (2002).

58. Cho, A. K. et al. Redox activity of airborne particulate matter at different sites in the Los Angeles Basin. *Environ. Res.* **99**, 40–47 (2005).

59. Vicedo-Cabrera, A. M. et al. Short term association between ozone and mortality: global two stage time series study in 406 locations in 20 countries. *BMJ* **368**, m108 (2020).

60. O'Brien, E. et al. Short-term association between sulfur dioxide and mortality: a multicountry analysis in 399 Cities. *Environ. Health Perspect.* **131**, 37002 (2023).

61. Ye, T. et al. Short-term exposure to wildfire-related PM(2.5) increases mortality risks and burdens in Brazil. *Nat. Commun.* **13**, 7651 (2022).

Author contributions

G.R.L, M.Z., and G.J. conceptualized the project and supervised the work. L.Q., G.R.L, and L.Y. designed the study and developed the methods. G.R.L, G.L., L.Q., H.Z., Q.L., and G.J. conducted PM sampling and coordinated the collection. L.Q., L.Y., and W.Z. performed the experiments. L.Q., G.R.L., L.L., and L.Y. collected, standardized, and analyzed the data. L.Q., G.R.L., and L.Y. wrote the original draft of the manuscript, which was reviewed and edited by S.T., Q.L., M.Z., and G.J. All authors were responsible for the decision to submit the manuscript.

Competing interests

The authors declare that they have no actual or potential competing financial interests or personal relationships that could appear to influence the work reported in this study.

Additional information

Supplementary information The online version contains supplementary material available at https://doi.org/10.1038/s41467-024-55151-8.

Correspondence and requests for materials should be addressed to Lili Yang or Guorui Liu.

Peer review information *Nature Communications* thanks Mohammed-noor Altarawneh, Jie Chen and Cong Liu for their contribution to the peer review of this work. A peer review file is available.

Reprints and permissions information is available at http://www.nature.com/reprints

Publisher's note Springer Nature remains neutral with regard to jurisdictional claims in published maps and institutional affiliations.